TYPE Original Research
PUBLISHED 17 March 2023
DOI 10.3389/fphot.2023.1081521

OPEN ACCESS

EDITED BY
Lei Kang,
The Pennsylvania State University (PSU), United States

REVIEWED BY
Arezou Rashidi,
University of Mazandaran, Iran
Domenico De Ceglia,
University of Brescia, Italy

*CORRESPONDENCE
Francesco Scotognella,
francesco.scotognella@polimi.it

SPECIALTY SECTION
This article was submitted to Optical Nanostructures, a section of the journal Frontiers in Photonics

RECEIVED 27 October 2022
ACCEPTED 03 March 2023
PUBLISHED 17 March 2023

CITATION
Scotognella F (2023), Vanadium oxide metal-insulator phase transition in different types of one-dimensional photonic microcavities.
Front. Photonics 4:1081521.
doi: 10.3389/fphot.2023.1081521

Vanadium oxide metal-insulator phase transition in different types of one-dimensional photonic microcavities

Francesco Scotognella*

Dipartimento di Fisica, Politecnico di Milano, Milan, Italy

The optical properties of vanadium dioxide (VO_2) can be tuned *via* metal-insulator transition. In this work, different types of one-dimensional photonic structure-based microcavities that embed vanadium dioxide have been studied in the spectral range between 900 nm and 2000 nm. In particular, VO_2 has been sandwiched between: i) two photonic crystals made of SiO_2 and ZrO_2; ii) two aperiodic structures made of SiO_2 and ZrO_2 that follow the Thue-Morse sequence; iii) two disordered photonic structures, made of SiO_2 and ZrO_2 in which the disorder is introduced either by a random sequence of the two materials or by a random variation of the thicknesses of the layers; iv) two four material-based photonic crystals made of SiO_2, Al_2O_3, Y_2O_3, and ZrO_2. The ordered structures i and iv show, respectively, one and two intense transmission valleys with defect modes, while the aperiodic and disordered structures ii and iii show a manifold of transmission valleys due to their complex layered configurations. The metal-insulator transition of VO_2, controlled by temperature, results in a modulation of the optical properties of the microcavities.

KEYWORDS

photonic cristals, vanadium oxide, metal-insulating transition, microcavities, transfer matrix method

Introduction

Crystalline vanadium dioxide (VO_2) shows a thermochromic phase transition around 68°C (341 K) (Morin, 1959). The phase transition is related to a structural crystal change from a monoclinic insulating phase to a tetragonal (rutile) metallic phase (Briggs et al., 2010; Currie et al., 2017). From an optical point of view, the phase transition of VO_2 results in a change from an insulating semi-transparent material to a metallic more lossy and reflective material (Verleur et al., 1968; Currie et al., 2017). The VO_2 phase transition can be exploited for several applications, such as smart windows, steep-slope devices for micro-electronics, neuromorphic computing devices, reconfigurable radiofrequency switches, optical limiters, and metasurfaces (Liu et al., 2018; Lu et al., 2021; Li et al., 2023; Tognazzi et al., 2023).

A method to utilize the VO_2 switchable optical properties is the integration of such material in photonic crystals (John, 1987; Yablonovitch, 1987; Joannopoulos, 2008). In photonic crystals, the periodic modulation of the refractive index in one, two or three dimensions gives rise to energy regions in which light is not transmitted through the crystal. The integration of materials with switchable optical properties in the infrared, such as photochromic polymers (Toccafondi et al., 2014) and infrared plasmonic nanomaterials

TABLE 1 Parameters of the Sellmeier equation for SiO_2, Al_2O_3, Y_2O_3, and ZrO_2.

Material	A_1	B_1	A_2	B_2	A_3	B_3	Ref
SiO_2	0.6961663	0.0684043	0.4079426	0.1162414	0.8974794	9.896161	Malitson, 1965; Tan (1998)
Al_2O_3	1.023798	0.0614482	1.058264	0.1106997	5.280792	17.92656	Malitson (1962)
Y_2O_3	2.578	0.1387	3.935	22.936	–	–	Nigara (1968)
ZrO_2	1.347091	0.062543	2.117788	0.166739	9.452943	24.32057	Wood and Nassau (1982)

(Guo et al., 2016; Kriegel et al., 2016), in one-dimensional photonic crystals has been proposed previously (Kriegel and Scotognella, 2018). Furthermore, the deposition of a VO_2 layer onto a one-dimensional photonic crystal has been theoretically studied by Rashidi et al. (2018) and experimentally studied by Singh et al. (Singh et al.(2020).

In this work, different types of one-dimensional photonic microcavities (Boucher et al., 2009) are proposed, in which a layer of VO_2 is embedded between two photonic crystals, two aperiodic Thue-Morse photonic structures, two disordered photonic structures, and two four-material based photonic crystals. The wavelength dependent refractive indexes of all the employed materials have been implemented. The light transmission of the microcavities has been simulated *via* the transfer matrix method. The modulation of the transmission spectra of the microcavities due the VO_2 metal-insulator phase transition has been highlighted.

Materials and methods

The light transmission of the different microcavities in the spectral range between 900 nm and 2000 nm has been studied with the transfer matrix method (Born et al., 1999; Xiao et al., 2016; Paternò et al., 2019). The system is glass/multilayer/air with light impinging the sample surface orthogonally. The characteristic matrix of the multilayer is written as

$$M = \begin{bmatrix} M_{11} & M_{12} \\ M_{21} & M_{22} \end{bmatrix} = \prod_{k=1}^{N} \begin{bmatrix} \cos\left(\frac{2\pi}{\lambda} n_k(\lambda) d_k\right) & -\frac{i}{n_k(\lambda)} \sin\left(\frac{2\pi}{\lambda} n_k(\lambda) d_k\right) \\ -i n_k(\lambda) \sin\left(\frac{2\pi}{\lambda} n_k(\lambda) d_k\right) & \cos\left(\frac{2\pi}{\lambda} n_k(\lambda) d_k\right) \end{bmatrix} \quad (1)$$

with k=(1,. . .,N) and N number of layers. The parameters d_k and $n_k(\lambda)$ are the thickness and the wavelength dependent refractive index of the kth layer, respectively. The light transmission is written as

$$T = \frac{n_0}{n_g} \left| \frac{2n_g}{(M_{11} + M_{12} n_0) n_g + (M_{21} + M_{22} n_0)} \right|^2 \quad (2)$$

with n_g the refractive index of glass and n_0 the refractive index of air ($n_g = 1.46$; $n_0 \cong 1$). The light transmission has been calculated in the selected spectral range with steps of 0.25 nm. The wavelength dependent refractive index $n_k(\lambda)$ can be written with the Sellmeier equation

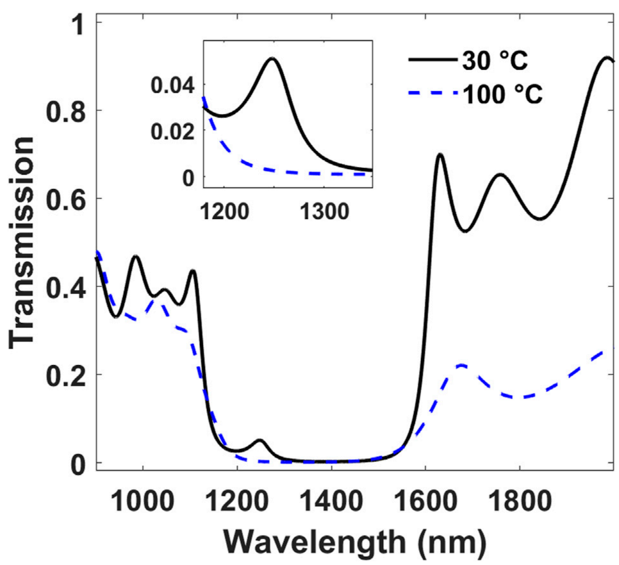

FIGURE 1
Light transmission spectra for the microcavity $(SiO_2/ZrO_2)_5/VO_2/(ZrO_2/SiO_2)_5$ with VO_2 in the insulating phase (at 30°C, black solid curve) and in the metallic phase (at 100°C, blue dashed curve).

$$n_k^2(\lambda) - 1 = \sum_{j'=1} \frac{A_{j'} \lambda^2}{\lambda^2 - B_j^2} \quad (3)$$

The parameters A_j and B_j are reported in Table 1.

The wavelength dependent refractive indexes of vanadium dioxide in the metal phase and in the insulating phase (30 °C) and in the metallic phase (100 °C) have been taken from Ref. (Briggs et al., 2010). The employment of the two refractive indexes in the transfer matrix method allows to simulate the optical properties of the different photonic structures in the two temperature regimes.

Results and discussion

In Figure 1 the light transmission spectrum for the microcavity $(SiO_2/ZrO_2)_5/VO_2/(ZrO_2/SiO_2)_5$ is shown. The black solid curve is related to VO_2 in the insulating phase, while the blue dashed curve is related to VO_2 in the metallic phase. The two phases correspond to a temperature of the material of 30°C for the insulating phase and a temperature of 100 °C for the metallic phase, respectively, as reported in Ref. (Briggs et al., 2010). In the microcavity the

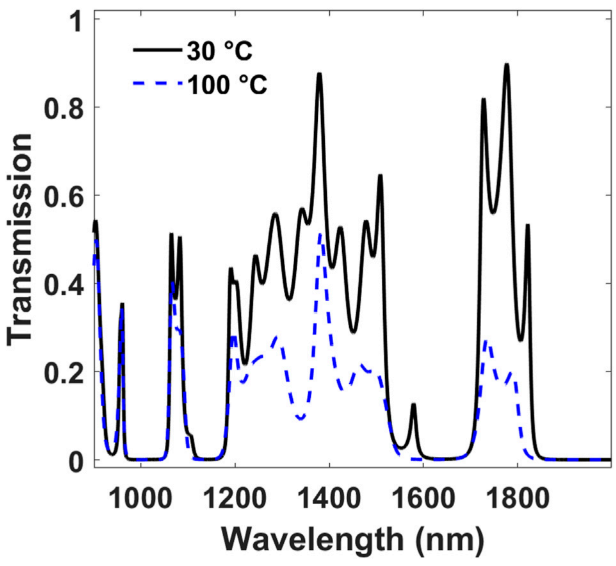

FIGURE 2
Light transmission spectra for the Thue-Morse aperiodic microcavity ABBABAABBAABABBABAABABBAABBABAAB/VO_2/ABBABAABBAABABBABAABABBAABBABAAB (A = SiO_2; B = ZrO_2) with VO_2 in the insulating phase (at 30°C, black solid curve) and in the metallic phase (at 100°C, blue dashed curve).

thickness of the silicon dioxide layers is 220 nm, the thickness of the zirconium dioxide layers is 165 nm, while the thickness of the vanadium dioxide layers is 55 nm.

In the microcavity configuration, the insulating VO_2 based microcavity shows a defect mode at around 1,250 nm within the photonic band gap of the structure (i.e., the intense transmission valley between 1,100 nm and 1,600 nm). The intensity of the defect mode is in agreement with experimental values shown in microcavities for coherent photoluminescence (Chiasera et al., 2019). On the other hand, for light filtering, the defect mode intensity is not high enough, and higher values are required for this type of application. The defect mode is magnified in the inset of Figure 1. Instead, for the metallic VO_2 based microcavity the defect mode is suppressed. Noteworthy, the transmission at wavelengths longer than 1,600 nm is weaker in the metallic VO_2 phase because of its infrared absorption.

In Figure 2 the transmission spectrum for the aperiodic microcavity that follows the Thue-Morse sequence is depicted. The VO_2 layer is sandwiched between two photonic structures with the sequence of layers ABBABAABBAABABBABAABABBAABBABAAB (Steurer and Sutter-Widmer, 2007) (A = SiO_2; B = ZrO_2). The layer thicknesses are the same ones of the periodic structure. The black solid curve is related to VO_2 in the insulating phase, while the blue dashed curve is related to VO_2 in the metallic phase. The transmission spectra are slightly modified with the VO_2 from the insulating to the metallic phase, with the suppression of peaks around 1,100 and 1,600 nm.

In Figure 3A the transmission spectra for the disordered microcavity, in which VO_2 is embedded between one-dimensional disordered photonic structures are shown (Wiersma et al., 2005; Wiersma, 2013). The proposed structure follows the sequence BBABBAABBBABBBBA/VO_2/BABAABBBBABBBABA. Also in this case, the layer thicknesses are the same ones of the periodic structure and the black solid curves correspond to the insulating phase of VO_2, while the blue dashed curves to the metallic phase of VO_2. The transmission spectrum with VO_2 in the insulating phase shows eight peaks in the studied range (900–2000 nm). With the transition from insulator to metal the suppression of most of the transmission peaks is noticeable.

In Figure 3B is shown the transmission spectra of the microcavity $(SiO_2/ZrO_2)_5/VO_2/(ZrO_2/SiO_2)_5$, in which a random variation of the thicknesses is introduced (Faist et al., 1989; Chiasera et al., 2015). For the SiO_2 layers the thickness follows $[2 \times (110 \pm n)]$, while for the ZrO_2 layers the thickness follows $[1.5 \times (110 \pm n)]$, where n is an integer random number between 0 and 20. The transmission spectrum for the microcavity with vanadium dioxide in the insulating phase shows a manifold of

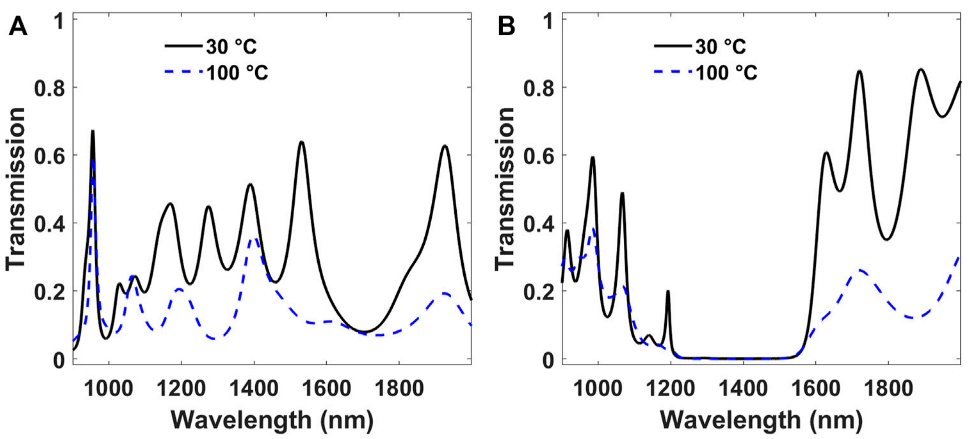

FIGURE 3
(A) Light transmission spectra for the disordered microcavity BBABBAABBBABBBBA/VO_2/BABAABBBBABBBABA (A = SiO_2; B = ZrO_2) with VO_2 in the insulating phase (at 30°C, black solid curve) and in the metallic phase (at 100°C, blue dashed curve). **(B)** Light transmission spectra for the microcavity $(SiO_2/ZrO_2)_5/VO_2/(ZrO_2/SiO_2)_5$, in which a random variation of the thicknesses is introduced, with VO_2 in the insulating phase (at 30°C, black solid curve) and in the metallic phase (at 100°C, blue dashed curve).

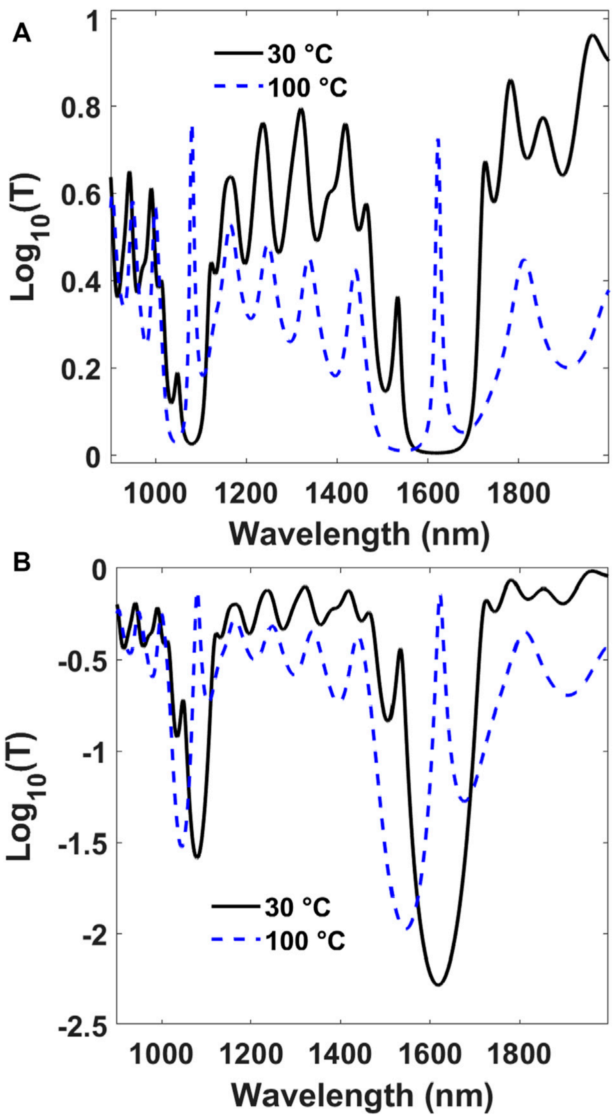

FIGURE 4
(A) Light transmission spectra for the four-material photonic crystal based microcavity $(SiO_2/Al_2O_3/Y_2O_3/ZrO_2)_6/VO_2/(ZrO_2/Y_2O_3/Al_2O_3/SiO_2)_6$ with VO2 in the insulating phase (at 30°C, black solid curve) and in the metallic phase (at 100°C, blue dashed curve). **(B)** Light transmission spectra for the four-material photonic crystal based microcavity in logarithmic scale.

transmission valleys and peaks. The transition from insulator to metal suppresses several transmission peaks, as, for example, the narrow peak at 1,200 nm.

In Figure 4A the transmission spectrum of the four material-based microcavity $(SiO_2/Al_2O_3/Y_2O_3/ZrO_2)_6/VO_2/(ZrO_2/Y_2O_3/Al_2O_3/SiO_2)_6$ is shown. The thickness of SiO_2 layers is 275.9 nm, the thickness of Al_2O_3 layers is 228.6 nm, the thickness of Y_2O_3 layers is 210.5 nm, the thickness of ZrO_2 layers is 190.5 nm, and the thickness of VO_2 layers is 45.9 nm. As shown in previous reports, four-material photonic crystals show a manifold of gaps (Kriegel and Scotognella, 2015). In fact, with this structure, in the wavelength interval between 900 nm and 2000 nm two intense photonic band gaps are observable, compared to the single photonic band gap of the microcavity (Figure 1). In this case, the defect modes of the two photonic band gaps show a red shift and a remarkable intensity increase. In Figure 4B the transmission spectrum of the four material-based microcavity is shown in logarithmic scale to highlight the large modulation depth of the transmission peak at around 1,100 nm and 1,600 nm for the metallic phases of vanadium dioxide.

Conclusion

In this work it has been studied the light transmission of different one-dimensional photonic microcavities that embed vanadium dioxide by means of the transfer matrix method. The four types of microcavities include periodic photonic crystals, aperiodic structures, disordered structures, and four-material-based photonic crystals. The different structures have been chosen in order to exploit their particular optical properties: An intense photonic bandgap with a defect for the microcavities including photonic crystals, a multiplicity of transmission valleys in the case of the microcavity with aperiodic structures, the occurrence of several transmission peaks, or a broader photonic band gap, in the case of microcavities with disordered structures, a doublet of photonic band gaps in the case of microcavities with four-material-based photonic structures. The transmission of VO_2 from insulator to metal, achievable *via* a temperature increase, leads to a modulation of the transmission spectra, noticeable with shifts and suppressions of transmission peaks. The modulation of the transmission spectra of the microcavities can be exploited for smart windows and temperature-controlled switches. Moreover, the photonic structure can be also used as temperature sensor since it has been studied by Currie et al. the temperature dependent refractive index dispersion of vanadium dioxide (Currie et al., 2017).

Data availability statement

The original contributions presented in the study are included in the article/supplementary material, further inquiries can be directed to the corresponding author.

Author contributions

FS is the sole author of the manuscript. FS conceived the idea, performed the simulations, analysed the data, wrote the manuscript.

Funding

This project has received funding from the European Research Council (ERC) under the European Union's Horizon 2020 research and innovation programme (grant agreement No. 816313).

Conflict of interest

The authors declare that the research was conducted in the absence of any commercial or financial relationships that could be construed as a potential conflict of interest.

Publisher's note

References

Born, M., Wolf, E., Bhatia, A. B., Clemmow, P. C., Gabor, D., Stokes, A. R., et al. (1999). *Principles of optics: Electromagnetic theory of propagation, interference and diffraction of light*. 7th ed. Cambridge, UK: Cambridge University Press. doi:10.1017/CBO9781139644181

Boucher, Y. G., Chiasera, A., Ferrari, M., and Righini, G. C. (2009). Photoluminescence spectra of an optically pumped erbium-doped micro-cavity with SiO2/TiO2 distributed Bragg reflectors. *J. Luminescence* 129, 1989–1993. doi:10.1016/j.jlumin.2009.04.085

Briggs, R. M., Pryce, I. M., and Atwater, H. A. (2010). Compact silicon photonic waveguide modulator based on the vanadium dioxide metal-insulator phase transition. *Opt. Express, OE* 18, 11192–11201. doi:10.1364/OE.18.011192

Chiasera, A., Meroni, C., Scotognella, F., Boucher, Y. G., Galzerano, G., Lukowiak, A., et al. (2019). Coherent emission from fully Er3+ doped monolithic 1-D dielectric microcavity fabricated by rf-sputtering. *Opt. Mater.* 87, 107–111. doi:10.1016/j.optmat.2018.04.057

Chiasera, A., Scotognella, F., Criante, L., Varas, S., Valle, G. D., Ramponi, R., et al. (2015). Disorder in photonic structures induced by random layer thickness. *Sci. Adv. mater* 7, 1207–1212. doi:10.1166/sam.2015.2249

Currie, M., Mastro, M. A., and Wheeler, V. D. (2017). Characterizing the tunable refractive index of vanadium dioxide. *Opt. Mater Express, OME* 7, 1697–1707. doi:10.1364/OME.7.001697

Faist, J., Ganière, J -D., Buffat, Ph, Sampson, S., and Reinhart, F -K. (1989). Characterization of $GaAs/(GaAs)_n(AlAs)_m$surface-emitting laser structures through reflectivity and high-resolution electron microscopy measurements. *J. Appl. Phys.* 66, 1023–1032. doi:10.1063/1.343488

Guo, P., Schaller, R. D., Ocola, L. E., Diroll, B. T., Ketterson, J. B., and Chang, R. P. H. (2016). Large optical nonlinearity of ITO nanorods for sub-picosecond all-optical modulation of the full-visible spectrum. *Nat. Commun.* 7, 12892–12892_10. doi:10.1038/ncomms12892

Joannopoulos, J. D. (Editor) (2008). *Photonic crystals: Molding the flow of light*. 2nd ed. (Princeton, NJ, USA: Princeton University Press).

John, S. (1987). Strong localization of photons in certain disordered dielectric superlattices. *Phys. Rev. Lett.* 58, 2486–2489. doi:10.1103/PhysRevLett.58.2486

Kriegel, I., and Scotognella, F. (2015). Band gap splitting and average transmission lowering in ordered and disordered one-dimensional photonic structures composed by more than two materials with the same optical thickness. *Opt. Commun.* 338, 523–527. doi:10.1016/j.optcom.2014.10.045

Kriegel, I., and Scotognella, F. (2018). Light-induced switching in pDTE–FICO 1D photonic structures. *Opt. Commun.* 410, 703–706. doi:10.1016/j.optcom.2017.11.019

Kriegel, I., Urso, C., Viola, D., De Trizio, L., Scotognella, F., Cerullo, G., et al. (2016). Ultrafast photodoping and plasmon dynamics in fluorine–indium codoped cadmium oxide nanocrystals for all-optical signal manipulation at optical communication wavelengths. *J. Phys. Chem. Lett.* 7, 3873–3881. doi:10.1021/acs.jpclett.6b01904

Li, B., Camacho-Morales, R., Li, N., Tognazzi, A., Gandolfi, M., Ceglia, D. de, et al. (2023). Fundamental limits for transmission modulation in VO_2 metasurfaces. *Phot. Res. PRJ* 11, B40–B49. doi:10.1364/PRJ.474328

Liu, K., Lee, S., Yang, S., Delaire, O., and Wu, J. (2018). Recent progresses on physics and applications of vanadium dioxide. *Mater. Today* 21, 875–896. doi:10.1016/j.mattod.2018.03.029

Lu, H., Clark, S., Guo, Y., and Robertson, J. (2021). The metal–insulator phase change in vanadium dioxide and its applications. *J. Appl. Phys.* 129, 240902. doi:10.1063/5.0027674

Malitson, I. H. (1965). Interspecimen comparison of the refractive index of fused silica. *J. Opt. Soc. Am. JOSA* 55, 1205–1209. doi:10.1364/JOSA.55.001205

Malitson, I. H. (1962). Refraction and dispersion of synthetic sapphire. *J. Opt. Soc. Am. JOSA* 52, 1377–1379. doi:10.1364/JOSA.52.001377

Morin, F. J. (1959). Oxides which show a metal-to-insulator transition at the neel temperature. *Phys. Rev. Lett.* 3, 34–36. doi:10.1103/PhysRevLett.3.34

Nigara, Y. (1968). Measurement of the optical constants of yttrium oxide. *Jpn. J. Appl. Phys.* 7, 404. doi:10.1143/JJAP.7.404

Paternò, G. M., Moscardi, L., Donini, S., Ariodanti, D., Kriegel, I., Zani, M., et al. (2019). Hybrid one-dimensional plasmonic–photonic crystals for optical detection of bacterial contaminants. *J. Phys. Chem. Lett.* 10, 4980–4986. doi:10.1021/acs.jpclett.9b01612

Rashidi, A., Hatef, A., and Namdar, A. (2018). On the enhancement of light absorption in vanadium dioxide/1D photonic crystal composite nanostructures. *J. Phys. D. Appl. Phys.* 51, 375102. doi:10.1088/1361-6463/aad70a

Singh, D. U., Bhoite, O., and Narayanan, R. (2020). Temperature tunable optical transmission using IR based 1D photonic crystals of VO_2 nanostructures. *J. Phys. D. Appl. Phys.* 53, 245106. doi:10.1088/1361-6463/ab7d69

Steurer, W., and Sutter-Widmer, D. (2007). Photonic and phononic quasicrystals. *J. Phys. D. Appl. Phys.* 40, R229–R247. doi:10.1088/0022-3727/40/13/R01

Tan, C. Z. (1998). Determination of refractive index of silica glass for infrared wavelengths by IR spectroscopy. *J. Non-Crystalline Solids* 223, 158–163. doi:10.1016/S0022-3093(97)00438-9

Toccafondi, C., Occhi, L., Cavalleri, O., Penco, A., Castagna, R., Bianco, A., et al. (2014). Photochromic and photomechanical responses of an amorphous diarylethene-based polymer: A spectroscopic ellipsometry investigation of ultrathin films. *J. Mater Chem. C* 2, 4692–4698. doi:10.1039/C4TC00371C

Tognazzi, A., Gandolfi, M., Li, B., Ambrosio, G., Franceschini, P., Camacho-Morales, R., et al. (2023). Opto-thermal dynamics of thin-film optical limiters based on the VO_2 phase transition. *Opt. Mater Express, OME* 13, 41–52. doi:10.1364/OME.472347

Verleur, H. W., Barker, A. S., and Berglund, C. N. (1968). Optical properties of VO2between 0.25 and 5 eV. *Phys. Rev.* 172, 788–798. doi:10.1103/PhysRev.172.788

Wiersma, D. S. (2013). Disordered photonics. *Nat. Photonics* 7, 188–196. doi:10.1038/nphoton.2013.29

Wiersma, D. S., Sapienza, R., Mujumdar, S., Colocci, M., Ghulinyan, M., and Pavesi, L. (2005). Optics of nanostructured dielectrics. *J. Opt. A: Pure Appl. Opt.* 7, S190–S197. doi:10.1088/1464-4258/7/2/025

Wood, D. L., and Nassau, K. (1982). Refractive index of cubic zirconia stabilized with yttria. *Appl. Opt. AO* 21, 2978–2981. doi:10.1364/AO.21.002978

Xiao, X., Wenjun, W., Shuhong, L., Wanquan, Z., Dong, Z., Qianqian, D., et al. (2016). Investigation of defect modes with Al2O3 and TiO2 in one-dimensional photonic crystals. *Optik* 127, 135–138. doi:10.1016/j.ijleo.2015.10.005

Yablonovitch, E. (1987). Inhibited spontaneous emission in solid-state physics and electronics. *Phys. Rev. Lett.* 58, 2059–2062. doi:10.1103/PhysRevLett.58.2059